EUROPEAN COOPERATION
IN THE FIELD OF SCIENTIFIC
AND TECHNICAL RESEARCH

EURO-COST

COST 2100 TD(10)12071
Bologna, Italy
2010/Nov/23-25

SOURCE: Department of Wireless Communications,
Faculty of Electrical Engineering and Computing,
University of Zagreb,
Croatia

Ray-tracing Study of Visibility Region Size in Urban Environment

Ana Katalinić[1,2], Radovan Zentner[2]
[1]Department of Wireless Communications
Faculty of Electrical Engineering and Computing
Unska 3
10000 Zagreb
CROATIA
Phone: + 385-01 61 29 712
Fax: + 385-01 61 29 717
Email: radovan.zentner@fer.hr
[2]Croatian and Electronic Communications Agency
Jurisiceva 13
10000 Zagreb
CROATIA
Phone: + 385-01 48 96 017
Email: ana.katalinic@hakom.hr

Ray-tracing Study of Visibility Region Size in Urban Environment

Ana Katalinic[1, 2], Radovan Zentner [2]

[1]*Croatian Post and Electronic Communications Agency*
Jurisiceva 13, Zagreb, Croatia
ana.katalinic@hakom.hr

[2]*University of Zagreb Faculty of Electrical Engineering and Computing*
Unska 3, Zagreb, Croatia
radovan.zentner@fer.hr

Abstract

The analysis of dynamics of change for multipath components along a route in urban environment is performed, in order to determine the size of visibility regions for multipath components. The analysis was performed using 3D ray tracing tool that calculated the direction of arrival, the length of each multipath component, as well as the power level for each ray. It was surprisingly observed that the size of visibility regions for most rays was at the level of one meter or less, so additional investigation is performed at this smaller scale. Shortness of visibility regions is discussed and explained through the nature of diffraction, which was dominant propagation mechanism in this investigation.

1. INTRODUCTION

Developing reference channel models (RCMs), which would describe realistic radio channel conditions as accurate as possible, has been a continuous challenge. Existing models are usually marked as either "stochastic", as their output comes from a stochastic process, or "deterministic", as they are based on real-life 3D topographic models of buildings in the area. Each group has its benefits and drawbacks, but it all comes to one thing: juggling between the accuracy and complexity.

In this paper we focus on modelling realistic scenario as accurate as possible, omitting the (computational) complexity for the time being. We focus on COST 273 [1] model, which is quite well established representation of Geometry Based Stochastic Channel Model (GBSCM) [1]-[6], but still lacks some specific parameter values. Particularly interesting is mimicking realistic multipath environments for a user mobile unit because it moves around. For tracking its position the model must handle appropriately the visibility of rays observed at a mobile unit, as the user, and keep the track of each ray along the route. In other words, the visibility region should be well defined.

Visibility Regions (VR), physical areas of coverage in which certain cluster is active or not, have been introduced in COST 259 model [5], [6], but remain rather unexplored. COST 259 model proposes to generate VR by Poisson process and suggests its size to be 100m in urban areas (and 300m in rural), but these values, to our knowledge, are not verified. In fact, as will be presented later in results, values obtained from our simulations were considerably shorter than proposed in COST 259: most of the rays were only one meter long or less. Motivated by those results, we performed

additional analysis of multipath dynamics within only one meter, keeping the track of the mobile station (MS) position every few centimetres.

Analyses have been performed using an accurate ray tracing (RT) simulator [8], [9] developed at University of Bologna (UniBO). The program implements a full-3D, full-vectorial ray tracing model in which also the diffused component of the field is computed with a statistical approach (the Effective Roughness approach). This tool enabled us also to present an insight into the number of rays typically present at the location, their type (line of sight – LOS, reflection, diffraction) and corresponding power distribution. Other topics such as delay and angular spread are quite well dealt with elsewhere [7]-[10].

Description of considered scenarios and presentation of results are given in two parts, corresponding to the "larger" and "smaller" scale analysis.

2. METHOD OF ANALYSIS

The set of rays originating from the transmitter (TX), passing through the same interactions and falling to the RX route we call one *ray entity* (RE). This ray entity must appear to the RX moving along the route, as a wave coming from one single source to all points at RX route where it is "visible" regardless the number of interactions since departing from TX. This is depicted in Fig. 1.

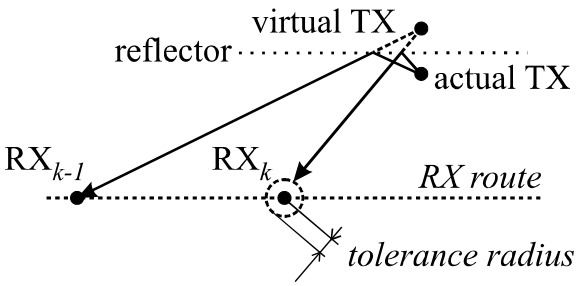

Fig. 1 In order to be in the same ray entity, two rays falling to two neighbouring RX locations must appear as if coming straight from same point in space (virtual TX)

For single (and double) reflected rays, the virtual source obtained as single (and double) mirror image of the TX represents a single source from where the rays within RE come from. However, conditions when diffraction occurs are somewhat different (see Fig. 2).

In case of diffraction, the virtual source (virtual TX) lies on the vertical corner edges of buildings, but unlike the reflection case where the virtual source location is fixed (see Fig. 1), the virtual source may slide along the edge (i.e. corner of the building), as we move RX location.

This is due to the Keller's cone condition [11], [12] as depicted in Fig. 2. For the same impinging wave, depending on the orientation of the RX route to the cone, we observe the drift of the virtual TX (e.g. points A, B, D along the route in Fig. 2) or not (in the vicinity of point C on the RX route in Fig. 2). In order to have static, fixed virtual TX in case of diffraction, route needs to be tangential to the Keller's cone.

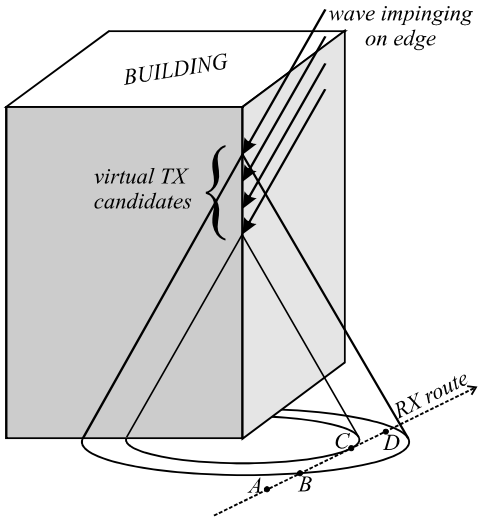

Fig. 2 Rays diffracted on vertical edge disperse along a cone, whose semi-angle equals to angle of incidence on the edge. Virtual TX varies along the RX route with minimum variation (practically fixed virtual TX) in the vicinity of point C (where route is tangent to the cone). In other points, where route cuts the cone (e.g. points A, B, D), virtual TX varies along the route

As will be seen from the results, most of the rays generated in our simulations contained at least one diffraction interaction (here diffraction is mainly connected to the *behind the corner* propagation). Since for most of the rays it is obviously more likely that RX route would cut cone rather than be tangent to it, it is to expect that most of the diffracted rays will last only a short length along the RX route. The results obtained in our calculations and presented later in the text confirmed this expectation.

For the processing of RT simulation results, we have developed an algorithm which tracks each ray from each RX, detects its counterparts from the same RE at each neighbouring RX location, thus following it from its beginning (the RX point where it appears) to its end (RX point where a ray disappears). The geometrical condition for two rays falling at the same angles of arrival (AoAs) at two neighbouring RX locations is given in Fig. 1. Here, an example of single reflection is given. Algorithm allows for a small tolerance depicted in Fig.1 as a small circle around RX_k. Tolerance value depends on the distance between two neighbouring RX, i.e. resolution (we used 1.5, 2 and 2.5 cm tolerance values in “large” scale simulations and 1.0, 2.0 and 3.0 mm in “small” scale case).

3. DESCRIPTION OF THE SCENARIO AND RESULTS

3.1 “Larger” scale analysis

Our test route (Fig. 3) was placed on the map of Stockholm. It was 200m long, from point A to point B, along one street. Transmitter antenna is omnidirectional (for generality) located as indicated (red). The transmitter was placed above the rooftop, so the whole scenario corresponds to the macro-cellular case, as defined in COST 259 model [5]. No line of sight was observed and also only a minor number of pure reflections.

We ran simulation for 200 receivers at height of 2m, with the distance between two adjacent receivers set to 1m. Preliminary investigation and simulations yielded that granulation of 1m is sufficient to observe the size of visibility regions with sufficient accuracy. This scenario actually describes the situation where the mobile station (MS) moves along a straight line (200m long) and we track changes every one meter.

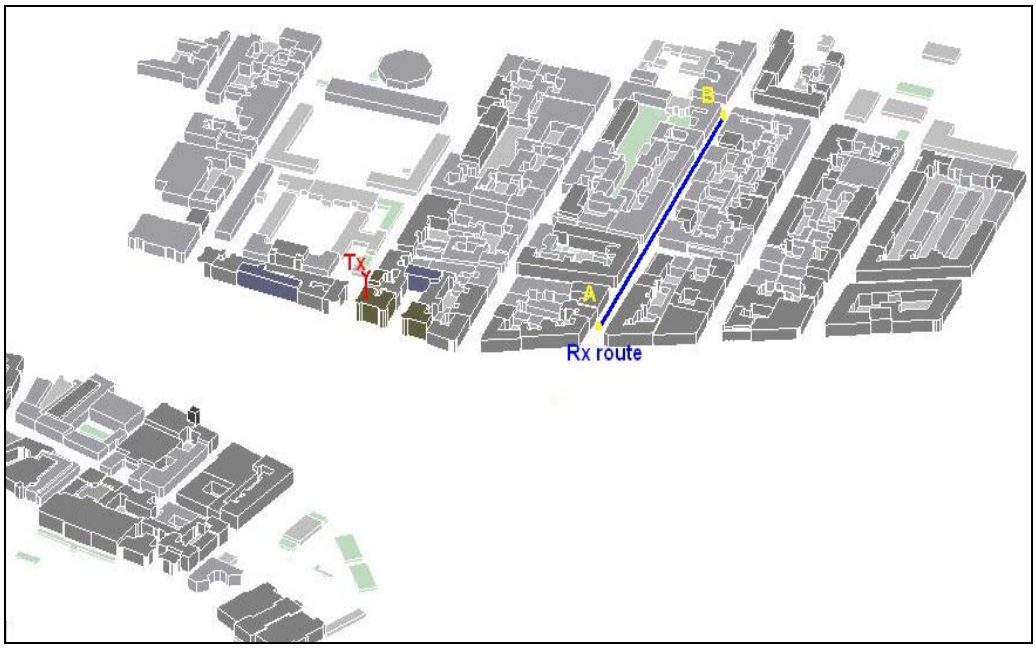

Fig. 3 Simulation scenario: a 200m long route in a street in Stockholm

The resulting number of calculated rays was around 15,000 with the number of rays at each RX ranging from 25 to 311. On average, that yields 76.91 rays per RX with dispersion of 58.71 rays. The number of considered rays was then reduced by imposing a power treshold. Power treshold of -150 dBW reduced the total power at the RX for negligible 0.03 dB on average (with dispersion of 0.067 dB) and maximal observed reduction at one RX for 0.76 dB. Table 1 presents decrease in number of rays due to this approximation.

TABLE 1
REDUCTION IN NUMBER OF CONSIDERED RAYS DUE TO POWER TRESHOLD

	Total # of rays	# of rays range @ RX	Average # of rays	Dispersion of # of rays
Raw rays data	15,382	From 25 to 311	76.91	58.71
Rays data after power treshold	2,243	From 1 to 39	11.21	9.88

Still, the number of rays per RX is large, impractical for detection through measurements, and unlikely to be fully exploited by either MIMO or diversity techniques, due to the antenna beam width constraints. In more detail, for the parametrization of stochastic channel models, it would be more appropriate to perform 3D spherical "convolution" with an idealised (for simplicity) of realistic RX antenna pattern (of e.g. 30°, 60°, 90° beam width). Here rays that fall within the radiation pattern should be summed up incoherently (since there is high likelihood that they will have mutually random phases), and thus obtained maxima would be actual *rays* which are visible, detectable and separable by the RX antenna. Still, in order to obtain physical insights as accurate as possible, in this paper we continue to use this large number of rays obtained by RT tool.

The chosen route for RX was not exposed to LOS, but also only a single point on the route (location 92 meters from the route start in point A, Fig. 4) could receive pure reflection from the walls. All other rays were either single/double diffractions, or mixed reflection/diffraction combinations.

Overall power and power attributed to these propagation methods was calculated at each RX site (every 1 meter along the route), summed incoherently (power sum) and presented in Fig. 4. The only reflection on the route (with significantly higher-than-average power) can also be seen. Note that

simulations were performed with idealistic omnidirectional antenna at TX (4π steradian), fed with 1W of power (0 dBW). Other power values in dB at the RX (Fig. 4, Table 2) are also in dBW, but W is omitted for the sake of clarity.

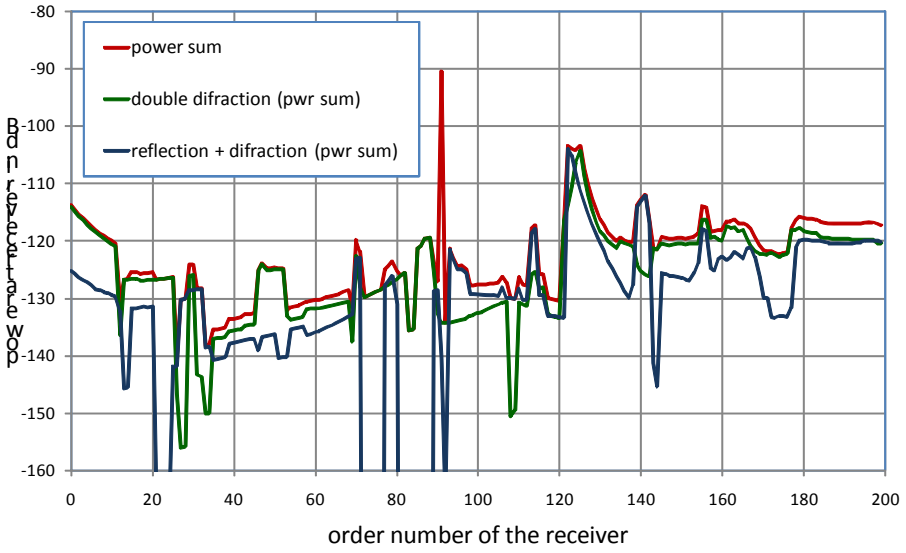

Fig. 4 Power of rays (non-coherent power sum) along the RX route. Total power at each RX is given (red), as well as its separate constituents, power of double diffracted rays (green) and mixed reflected + diffracted rays. No LOS rays were present and only one pure reflection (the peak in the total power, at RX location 92)

Table 2 gives frequencies of occurrence of ray entities with sizes from 1m to 11m long (the longest observed length was 11m). One can see that negligible amount of rays or power (only 0.81%) is actually present in entities longer than 1m. Even if we adjust the data by ignoring the large reflection ray on RX location #92 (Fig. 4) still only 2.7% of power is in rays longer than 1m.

TABLE 2

DATA OF OBSERVED RAY ENTITIES ALONG THE RX ROUTE DEPICTED IN FIG. 3

	number of entities along the route			total power within the entity set (in dB)		
tolerance	1.5 cm	2.0 cm	2.5 cm	1.5 cm	2.0 cm	2.5 cm
entity length: 11m	1	1	1	-122.0	-122.0	-122.0
entity length: 10m	0	0	3	---	---	-123.1
entity length: 9m	1	2	1	-139.7	-127.0	-139.7
entity length: 8m	0	3	4	---	-126.6	-115.9
entity length: 7m	0	5	7	---	-114.1	-116.6
entity length: 6m	2	2	4	-131.3	-124.1	-121.9
entity length: 5m	1	4	5	-136.3	-122.8	-122.2
entity length: 4m	0	10	7	---	-122.2	-120.9
entity length: 3m	2	7	6	-135.4	-123.1	-125.8
entity length: 2m	14	30	36	-117.7	-118.0	-116.9
entity length: 1m	1975	1805	1748	-89.0	-89.0	-89.0

These data call for serious reconsideration of modeling visibility regions in stochastic channel models such as COST 259 model, since it illustrates that these visibility regions would be rather short. Alternatively, if in the stochastic channel model with twin-clusters (COST 259 model) one would incorporate possibility that virtual source (virtual TX) within the cluster would change its altitude as the RX moves along the route, thus taking into account this foreseen property of diffracted rays, much larger and more reasonable visibility regions could be detected. Judging on the basis of maximum visibility region size detected here and presented in Table 2, sizes of 10m or larger visibility regions could be appropriately adjusted in COST 259 model. Still, for this further investigation would be required.

3.2 "Smaller" Scale

Since most of the total power lies in short (mostly diffracted) rays with length less than 1 meter, we did additional investigation on a smaller scale. We ran simulations over a 1 meter route in 20 different points (i.e. keeping the track of the MS position every 5 cm). For the purpose of analysis and comparison, this 1 m route is actually a part of the same route we used in the first run (Fig. 5).

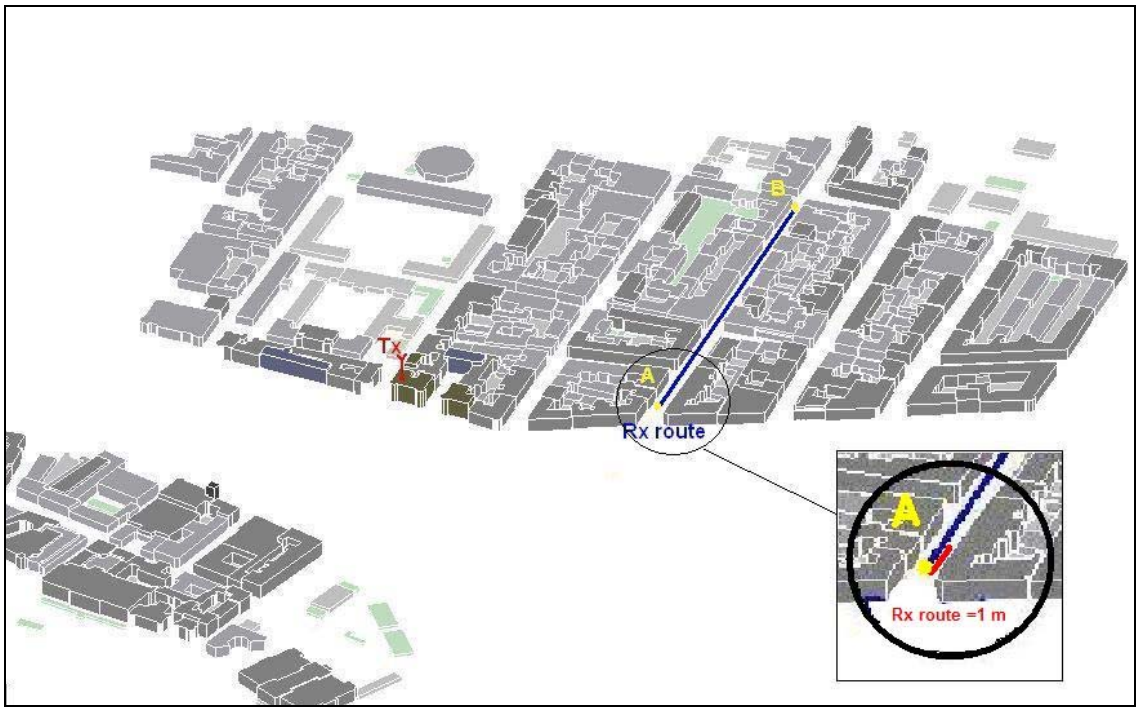

Fig. 5 Simulation scenario: 1 meter long route along the street in Stockholm

In order to decrease the simulation time, the number of rays considered was reduced to those with power level above the previously introduced threshold of -150 dBW. Since this mini route is actually part of the larger route and part of the same radio environment, it can be assumed that overall influence of weaker rays can be neglected.

The number of calculate rays on this route was around 200, with most RX having 10 rays, except one (#8, i.e. 0.4 m) with 11 rays and the last one (#20, i.e. 1.0 m) with only one ray. Table 3 gives frequencies of occurrence of ray entities with different sizes and appropriate power levels. In first two cases (tolerance values 1.0 and 2.0 mm), most power lies in huge number of very short ray entities (100% and 86% respectively is in ray entities of 5 cm). In 3rd case, when more than one "longer" ray entity is present, more than half of power (around 55%) is in the longest ray entities of

0.6 m. This result requires further studies on small scale levels and appropriate resolution, but also some more investigation on ray detection algorithms.

TABLE 3
DATA OF OBSERVED RAY ENTITIES ALONG THE RX ROUTE DEPICTED IN FIG. 5

	number of entities along the route			total power within the entity set (in dB)		
Tolerance	1.0 mm	2.0 mm	3.0 mm	1.0 mm	2.0 mm	3.0 mm
entity length: 60cm	---	1	6	---	-132.777	-104.098
entity length: 50cm	---	---	---	---	---	---
entity length: 45cm	---	---	---	---	---	---
entity length: 40cm	---	1	4	---	-137.493	-105.443
entity length: 35cm	---	---	1	---	---	-129.591
entity length: 30cm	---	---	---	---	---	---
entity length: 25cm	---	---	1	---	---	-131.047
entity length: 20cm	---	1	2	---	---	-132.437
entity length: 15cm	---	---	5	---	---	-128.621
entity length: 10cm	17	27	34	---	-134.894	-119.956
entity length: 5cm	159	109	29	-101.696	-102.171	-117.761

4. CONCLUSIONS

Our results show that duration of rays along the path (visibility region) in urban scenarios is much shorter than commonly expected. Most of them last less than 1 meter and from the smaller scale we can notice some rays which last only few centimeters. Only a few last for just above 10m. Even more interestingly, in total, not much power is present in the longer-lasting rays. This is in conflict with until now published opinions (e.g. COST 259 model) that rays are visible for roughly 100m (urban scenario) or up to 300m (rural scenario). Although our results are obtained on only one single urban area, we can conclude that visibility regions as conceived in COST 259 model should maybe be somewhat revised.

One pattern that we noticed is that if we would expand the tolerance for the identification of rays, by allowing the vertical component of virtual TX to slide, longer ray durations would be observed. Also we noticed that much higher number of rays is detected using RT than typically measured using standard equipment as MIMO channel sounders. So we come to two interesting directions for further research. One is to treat diffraction rays separately as entity rays, with modification of virtual TX z-coordinate along the duration path. This feature should also be included in the stochastic model. The other is to perform 3D spherical “convolution“ with an idealized (for simplicity) of realistic RX antenna pattern (of e.g. 30°, 60°, 90° beam width). Here, rays that fall within the radiation pattern should be summed up incoherently (since there is high likelihood that they will have mutually random phases), and thus obtained maxima would be actual “rays“ visible, detectable and separable by the RX antenna. Visibility length of such “rays“ would for sure be longer, yet these “rays“ should have some variation (continuous) in amplitude and phase along the visibility area, statistics of which is yet to be investigated.

ACKNOWLEDGMENT

The authors wish to thank Professor Vittorio Degli-Esposti and Enrico Maria Vittucci from the University of Bologna (UniBO) for kindly allowing us to use a 3D ray tracing tool developed at UniBO, as well as the digital map of Stockholm provided by Ericsson AB.

REFERENCES

[1] L. Correia, Ed., *Mobile Broadband Multimedia Networks*, COST 273 final report, Elsevier Science Publishers B.V., 2006.

[2] B.W.M. Kuipers, M. Mackowiak, L.M. Correia, "Understanding Geometrically based Multiple Bounce Channel Models", The Second European Conference on Antennas and Propagation, EuCAP 2007. pp. 1 – 4

[3] P. Kyösti et al., WINNER II Channel Models, Deliverable D1.1.2 V1.1, November 2007 (www.ist-winner.org/)

[4] H. Hofstetter, A. Molisch, N. Czink, "A twin-cluster MIMO channel model", *The First European Conference on Antennas and Propagation, EuCAP 2006*. pp. 1 – 4

[5] A. F. Molisch, H. Asplund, R Heddergott, M. Steinbauer, T. Zwick, "The COST 259 Directional Channel Model-Part I: Overview and Methodology", *IEEE Transactions on Wireless Communications*, Volume 5, Issue 12, pp:3421 – 3433, Dec. 2006

[6] H. Asplund, A.A. Glazunov, A.F. Molisch, K.I. Pedersen, M. Steinbauer, "The COST 259 Directional Channel Model-Part II: Macrocells", *IEEE Transactions on Wireless Communications*, Volume 5, Issue 12, pp:3434 - 3450 , Dec. 2006

[7] F. Quitin, C. Oestges, F. Horlin, and P. De Doncker, "Multipolarized MIMO Channel Characteristics: Analytical Study and Experimental Results", *IEEE Transactions on Antennas and Propagation*, Volume 57, Issue 9, pp:2739 – 2745, Dec. 2009

[8] V. Degli-Esposti, D. Guiducci, A. de'Marsi, P. Azzi, F. Fuschini, "An advanced field prediction model including diffuse scattering", *IEEE Transactions on Antennas and Propagation*, Volume 52, Issue 7, pp:1717 – 1728, Jul. 2004

[9] V. Degli-Esposti, F. Fuschini, E.M. Vitucci, G. Falciasecca, "Speed-Up Techniques for Ray Tracing Field Prediction Models", *IEEE Transactions on Antennas and Propagation*, Volume 57, Issue 5, pp:¸1469 – 1480, May 2009

[10] F. Fuschini, H. El-Sallabi, V. Degli-Esposti, L. Vuokko, D. Guiducci, P. Vainikainen, "Analysis of Multipath Propagation in Urban Environment Through Multidimensional Measurements and Advanced Ray Tracing Simulation", *IEEE Transactions on Antennas and Propagation*, Volume 56, Issue 3, pp:¸ 848 – 857, Mar. 2008

[11] J.B. Keller, "Geometrical Theory of Diffraction", *J. Opt. Soc. of America*, Vol. 52, No.2, pp. 116-130, Feb. 1962

[12] D.A. McNamara, C.W.I. Pistorius, J.A.G. Malherbe, *Introduction to the Uniform Geometrical Theory of Diffraction,* Artech House, Boston London, 1990